Sound field synthesis of a moving virtual sound source applying the Spectral Division Method

G. Firtha[1], **P. Fiala**[1]
[1]Budapest University of Technology and Economics, Department of Networked Systems and Services, Magyar Tudósok körútja 2, H-1117, Budapest, Hungary
e-mail: **firtha@hit.bme.hu**

Abstract
Sound field reproduction is a state-of-the-art technique, aiming to physically reproduce the sound field of a virtual sound source. To achieve this, a densely spaced loudspeaker array, termed as secondary source distribution is driven by a driving function derived either in spatial or spectral domain. The former is termed as Wave Field Synthesis (WFS), while the latter is called the Spectral Division Method (SDM). The synthesis of the sound field generated by a moving virtual sound source has been subject of extensive research in the recent decade. However, only spatial domain solutions, based on the theory of WFS are known so far. Our paper presents a new modeling approach, based entirely on the wavenumber-frequency domain description of the moving virtual sound source. For a moving sound source both temporal and spatial Fourier-transforms can be found analytically. By utilizing the SDM the spatial-frequency domain epxression for the loudspeaker driving function can be given explicitly. We show that – in contrary to other approaches - the proposed method results in analytically correct driving functions, which ensure perfect synthesis on a reference line.

1 Introduction

The perfect physical reconstruction of a desired sound field has been target of extensive research in the last two decades. The aim of these systems is to physically reproduce a targeted sound field in an extended listening area The synthesis is performed by using an arrangement of loudspeakers, called secondary sources. The objective of sound field reproduction is to find the driving signals of the secondary sources in order to obtain the desired field as the superposition of their individual sound fields. The target sound field is most often a plane wave or the field evoked by a point source, whereas the loudspeaker arrangement is a linear, planar, circular or spherical distribution. Several techniques exist to find the loudspeaker driving functions in both analytical and numerical manner. In the current treatise only analytical approaches are taken into consideration, applying linear secondary source distribution.

In the case of linear or planar secondary sources the most prominent technique is wave field synthesis (WFS), based on the Rayleigh-integral formulation of the wave field emitted by the virtual sound source [5, 12, 14]. For circular and spherical distributions most techniques rely on a mode-matching solution, performed in the spherical harmonic domain, originating from the traditional Ambisonics technique [1, 4, 3]. Besides the WFS an Ambisonic-like mode-matching solution—termed the spectral division method (SDM)—has been recently introduced [10, 3], which solves the problem in the spectral (wavenumber) domain.

Besides the sound field reproduction of stationary sources the synthesis of moving sound sources has gained an increasing interest. A typical example application is the synthesis of dynamic sound-scenes in virtual reality or cinema sound systems. For moving sound sources the proper reconstruction of the Doppler effect is of primary importance.

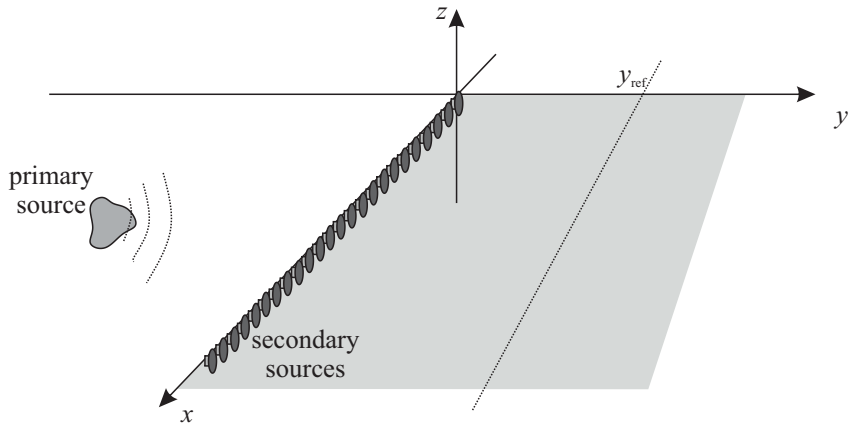

Figure 1: Arrangement for synthesis of arbitrary sound field by applying a linear secondary source distribution

Early implementations of the WFS with moving sources simulate the source motion as a sequence of stationary positions. The technique ends up in a Doppler-like frequency variation, however, the generated sound field suffers from several artifacts. Besides the deviation from the physically correct Doppler-frequency shift, a spectral broadening arises, which makes the correct synthesis of an arbitrary wave front infeasible [7]. A recent approach attempts to incorporate the physical description of the dynamics of the moving sound source into 3D WFS [9, 3]. The method provides mathematically correct time-domain driving functions for planar secondary sources. However, for linear secondary source distribution a mathematically inconsistent solution is presented by applying frequency-domain approximations in the time-domain.

The present paper revisits the synthesis of sound fields emitted by uniformly moving sound sources. After a short overview on the theory of WFS and SDM, as a basis for the synthesis equations analytical formulation is given both in spatio-spectral and wavenumber-spectral domain for a uniformly moving source, moving at an arbitrary direction. By applying the traditional WFS approximations, and in the spectral domain, using SDM explicit analytical driving functions are given in order to synthesize a moving virtual source, oscillating harmonically.

2 Principles of sound field reconstruction

Before investigating the description of moving sound sources the basic theory of sound field reconstruction is outlined. The general arrangement used throughout this paper is shown in Fig. xy. An infinite linear distribution of identical, shift-invariant secondary point sources, located along the $[x\ 0\ 0]^{\mathrm{T}}$ axis is considered.

The spectrum of the synthesized sound field $P(\mathbf{x}, \omega)$ at $\mathbf{x} = [x\ y\ z]^{\mathrm{T}}$ can be written as the weighted sum of the field of the secondary source elements

$$P(x, y, z, \omega) = \int_{-\infty}^{\infty} D(x_0, \omega) G(x - x_0, y, z, \omega) \mathrm{d}x_0, \tag{1}$$

where $G(\mathbf{x}, \omega)$ denotes the transfer function of a secondary source element from the origin to the listener position, while $D(x_0, \omega)$ denotes the driving function for the secondary source element located at x_0. Note, that the equation does not have any restriction for the elements of secondary source distribution. For 3D problems secondary source elements are most often modeled as acoustic monopoles, where

$$G_{3\mathrm{D}}(x, y, z, \omega) = \frac{1}{4\pi} \frac{\mathrm{e}^{-\mathrm{j}k|\mathbf{x}|}}{|\mathbf{x}|} \tag{2}$$

is the 3D full space Green's function. Our aim is to find the driving function, so that the integral will equal to the targeted sound field, thus an inverse problem has to be solved.

2.1 Wave field synthesis

The traditional solution for the problem is termed as Wave Field Synthesis. The basis of WFS is the Rayleigh-integral formulation of an arbitrary sound field. The Rayleigh-I integral states that any sound field, generated by an arbitrary source distribution in the half space $y < 0$ can be described in $y > 0$ merely using boundary conditions, by weighting a continuous monopole distribution with the normal velocity, generated on the boundary plane $y = 0$ [14]:

$$P(\mathbf{x},\omega) = -2 \iint_{-\infty}^{\infty} \left. \frac{\partial P(\mathbf{x},\omega)}{\partial y} \right|_{y=0} G_{3\mathrm{D}}(\mathbf{x}-\mathbf{x}_0,\omega)\mathrm{d}x_0\mathrm{d}z_0. \tag{3}$$

The Rayleigh integral thus explicitly contains the driving function, for a planar secondary source distribution, which is the normal derivative of the targeted sound field at the secondary sources. The solution would provide a perfect synthesis in the $y > 0$ half space. Note, that the Rayleigh-integral provides correct result only for the case of monopole secondary sources.

Traditionally, in order to obtain the driving functions for a linear secondary array, the stationary-phase method [11] is applied to integral (3). The method is based on the approximation of rapidly oscillating functions using a second order Taylor series, followed by analytical integration along the z axis [5, 14]. Similar approximations was presented by Spors et al. by applying a secondary source correction term [12], however for the case of moving secondary sources only the traditional approach can be used, as it will be seen later.

As the result of the approximation, phase-correct synthesis is restricted to the *synthesis plane*, i.e. the horizontal plane containing the virtual sound source and the secondary source distribution. Furthermore, amplitude correct synthesis is restricted to the *reference line*, parallel to the secondary source.

2.2 Spectral division method

The less physical alternative for WFS relies on the fact that integral (1) can be recognized as a convolution along the secondary source distribution along the x-dimension. By applying a Fourier-transform along the x-axis, the wave number domain representation $\tilde{P}$ of the synthesized field is obtained in the form of a spectral product. Throughout the present research the spatial Fourier-transform was defined by

$$\tilde{P}(k_x, y, z, \omega) = \int_{-\infty}^{\infty} P(\mathbf{x},\omega)\mathrm{e}^{\mathrm{j}k_x x}\mathrm{d}x, \tag{4}$$

$$P(\mathbf{x},\omega) = \frac{1}{2\pi}\int_{-\infty}^{\infty} \tilde{P}(k_x, y, z, \omega)\mathrm{e}^{-\mathrm{j}k_x x}\mathrm{d}k_x. \tag{5}$$

Specifically, the desired field on the reference line can be formulated as

$$\tilde{P}(k_x, y_{\mathrm{ref}}, 0, \omega) = \tilde{D}(k_x,\omega)\tilde{G}(k_x, y_{\mathrm{ref}}, 0, \omega). \tag{6}$$

and the driving functions are computed by a spectral division:

$$\tilde{D}(k_x,\omega) = \frac{\tilde{P}(k_x, y_{\mathrm{ref}}, 0, \omega)}{\tilde{G}(k_x, y_{\mathrm{ref}}, 0, \omega)}. \tag{7}$$

The SDM employs no approximation, ensures perfect synthesis on the reference line, and can be therefore regarded as a reference solution. However, direct applications require the inverse-transform of the driving

function $\tilde{D}$, which often can't be calculated analytically (e.g. for a virtual point source in a stationary position).

Again, note that in this case there's no restriction on the field of the secondary source elements, the approach is applicable with arbitrary secondary source radiation properties. In the present research as for WFS here also acoustic monopoles were assumed as secondary source elements, thus the spatial Fourier transform of expression (2) is needed.

Using the Euler's formula and [8, (3.876-1,2)] the spectrum is given by [10]. We may use that $\sqrt{k^2-k_x^2}r_t = -\mathrm{j}\sqrt{k_x^2-k^2}r_t$, where $r_t = \sqrt{y^2+z^2}$ is the transversal distance:

$$\hat{G}_{3\mathrm{D}}(k_x,y,z,\omega) = \begin{cases} -\frac{\mathrm{j}}{4}H_0^{(2)}\left(-\mathrm{j}\sqrt{k_x^2-k^2}r_t\right), & |k_x| \leq |k| \\ \frac{1}{2\pi}K_0\left(\sqrt{k_x^2-k^2}r_t\right), & |k| \leq |k_x|. \end{cases}$$

By considering that $\arg\left(\sqrt{k_x^2-k^2}r_t\right) = 0$ for the evanescent or $\frac{\pi}{2}$ for the propagating part, we can use [2, (9.6.4)], thus the spectrum of sound source can be written either by the Hankel function or the modified Bessel function:

$$\hat{G}_{3\mathrm{D}}(k_x,y,z,\omega) = -\frac{\mathrm{j}}{4}H_0^{(2)}\left(-\mathrm{j}k_t r_t\right) = \frac{1}{2\pi}K_0\left(k_t r_t\right), \tag{8}$$

with $k_t = \sqrt{k_x^2-k^2}$ denoting the transversal wavenumber.

3 Description of moving sources

3.1 Rayleigh-integral for moving sources

The approaches presented in the previous section may be applied to arbitrary target sound fields. Application of the WFS requires the normal derivative of the desired field on the boundary plane, while for SDM the frequency-wavenumber formulation of the pressure field on the reference line is needed for synthesis. In the present chapter the descripition of the target sound field, the field of a moving acoustic point source is formulated first in frequency-spatial, then in the frequency-wavenumber domain, and also the equivalent Rayleigh-integral description is given.

In the derivation only sources moving parallel to the x-axis are considered. A translation invariant sound source traveling along line $[x, y_\mathrm{s}, 0]^\mathrm{T}$ with a uniform subsonic velocity v is assumed. The source is located at $[x_\mathrm{s}\ y_\mathrm{s}\ 0]^\mathrm{T}$ at the time origin, as shown in Fig. 2.

The description of the time history of the sound field, generated by the moving source can be written as a convolutional integral, as it was also given in [3]. Consider a harmonically oscillating source located at $\mathbf{x}_s(\tau) = [x_s + v\tau, y_s, z_s]^\mathrm{T}$ radiating with a source time history $q(\tau) = \mathrm{e}^{\mathrm{j}\omega_0\tau}$. The sound field can be expressed as the response of a linear time-variant system with a time-varying impulse response $g_\mathrm{m}(\mathbf{x} - \mathbf{x_s}(\tau), \tau)$:

$$p_\mathrm{m}(\mathbf{x},t) = \int_{-\infty}^{\infty} g_\mathrm{m}(x-x_s-v\tau, y-y_s, z-z_s, t-\tau)q(\tau)\mathrm{d}\tau. \tag{9}$$

Substituting $q(\tau)$, performing a forward Fourier transform with respect to time and expressing the source impulse response g_m with its wavenumber-frequency domain representation $\tilde{G}_m(k_x,y,z,\omega)$ yields

$$P_\mathrm{m}(\mathbf{x},\omega) = \underset{(t)}{\int}\underset{(\tau)}{\int}\underset{(\omega')}{\int}\underset{(k_x)}{\int} \frac{1}{4\pi^2}\tilde{G}_\mathrm{m}(k_x, y-y_s, z-z_s, \omega') \\ \mathrm{e}^{-\mathrm{j}k_x(x-x_s-v\tau)}\mathrm{d}k_x\mathrm{e}^{\mathrm{j}\omega'(t-\tau)}\mathrm{d}\omega'\mathrm{e}^{\mathrm{j}\omega_0\tau}\mathrm{d}\tau\mathrm{e}^{-\mathrm{j}\omega t}\mathrm{d}t \tag{10}$$

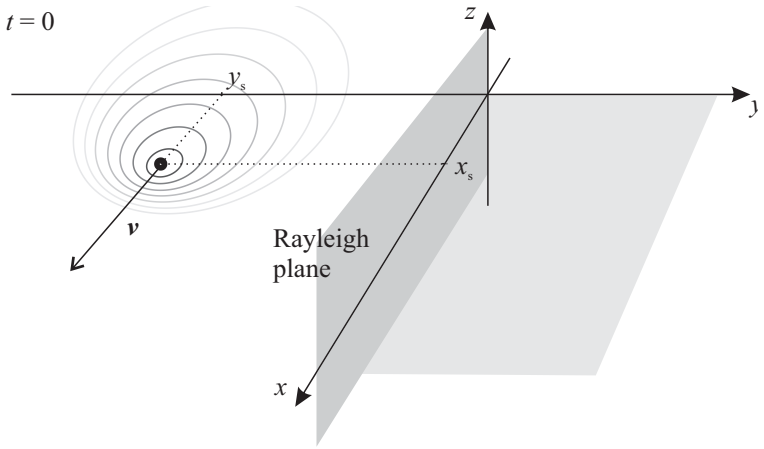

Figure 2: Arrangement for description of a moving sound source

Reversing the order of integration, and simplifying the Fourier transform of exponentials:

$$P_{\mathrm{m}}(\mathbf{x},\omega) = \int\limits_{(\omega')}\int\limits_{(k_x)} \frac{1}{4\pi^2}\tilde{G}_{\mathrm{m}}(k_x, y-y_s, z-z_s, \omega')\mathrm{e}^{-\mathrm{j}k_x(x-x_s)} \int\limits_{(t)} \mathrm{e}^{-\mathrm{j}(\omega-\omega')t}\mathrm{d}t \int\limits_{(\tau)} \mathrm{e}^{\mathrm{j}(k_x v-(\omega'-\omega_0))\tau}\mathrm{d}\tau\mathrm{d}k_x\mathrm{d}\omega' \quad (11)$$

$$P_{\mathrm{m}}(\mathbf{x},\omega) = \int\limits_{(\omega')}\int\limits_{(k_x)} \frac{1}{4\pi^2}\tilde{G}_{\mathrm{m}}(k_x, y-y_s, z-z_s, \omega')\mathrm{e}^{-\mathrm{j}k_x(x-x_s)}\delta(\omega-\omega')\delta(vk_x-(\omega'-\omega_0))\mathrm{d}k_x\mathrm{d}\omega' \quad (12)$$

By exploiting the sifting property of Dirac-delta and the rescaling theorem we arrive to the final result:

$$P_{\mathrm{m}}(\mathbf{x},\omega) = \frac{1}{v}\tilde{G}_{\mathrm{m}}\left(\hat{k}, y-y_s, z-z_s, \omega\right)\mathrm{e}^{-\mathrm{j}\hat{k}(x-x_{\mathrm{s}})}. \quad (13)$$

where $\hat{k} = \frac{\omega-\omega_0}{v}$.

In the aspect of WFS the Rayleigh-integral for moving sources is of great interest. The plane for which the integral is written can be seen in figure 2. Substituting (13) into (3), the following Rayleigh integral is obtained for the pressure field of the harmonic moving source:

$$P_m(\mathbf{x},\omega) = -\frac{2}{v}\iint_{-\infty}^{\infty}\frac{\partial}{\partial y}\tilde{G}_{\mathrm{m}}\left(\hat{k}, y-y_s, z_0-z_s, \omega\right)\Big|_{y=0}\mathrm{e}^{-\mathrm{j}\hat{k}(x_0-x_{\mathrm{s}})}G_{3\mathrm{D}}(x-x_0, y, z-z_0, \omega)\mathrm{d}x_0\mathrm{d}z_0. \quad (14)$$

An interesting property of the Rayleigh-integral (14) for a moving source is that the integration with respect to x_0 can be carried out analytically. It can be considered as the Fourier transform of the secondary sources' Green's function $G_{3\mathrm{D}}$. The resulting simplified integral reads:

$$P_m(\mathbf{x},\omega) = \frac{-2}{v}\int\limits_{(z_0)}\frac{\partial\tilde{G}_m(\hat{k}, y_0-y_s, z_0, \omega)}{\partial y_0}\Big|_{y_0=0}\tilde{G}_{3\mathrm{D}}(\hat{k}, y, z-z_0, \omega)\mathrm{d}z_0\mathrm{e}^{-\mathrm{j}\hat{k}(x-x_s)}. \quad (15)$$

The equation states that the field generated by a moving source equals to the field of a vertical set of monopoles moving with the same velocity v and driven with two times the normal velocity, that the original source would generate at $[0,0,z]^{\mathrm{T}}$.

From here let's assume that not only the secondary source elements, but also the moving source is an acoustic point source, meaning $g_{\mathrm{m}}(\cdot) = g(\cdot)$ (omitting the 3D subscript). For such a point-source the temporal

spectrum is given in (2) and the spatio-temporal spectrum is give in (8), thus with substituting $k_x = \hat{k}$ the spectrum of the moving source is given by

$$P_{\mathrm{m}}(\mathbf{x},\omega) = -\frac{\mathrm{j}}{4v} H_0^{(2)}(-\mathrm{j}\hat{k}_t r_t)\mathrm{e}^{-\mathrm{j}\hat{k}(x-x_{\mathrm{s}})}, \tag{16}$$

where $\hat{k}_t = \sqrt{\hat{k}^2 - k^2}$, $k = \frac{\omega}{c}$ is the wavenumber and again, $\hat{k} = \frac{\omega-\omega_0}{v}$ is a shifted wavenumber.

The pertinence of equations (14) and (15) can be verified by applying a further spatial Fourier-transform in the z-direction using formulation given by [15, 3], so that convolution given in (15) can be carried out. As a result we obtain exactly the field, generated by the original moving source.

The physical interpretation of the radiated field by a moving source (13) is the following: The time history overgoes only a temporal shift by a factor of $\frac{x-x_s}{v}$ and the phase change of $\omega_0 \frac{x-x_s}{v}$ along the x axis, and its main characteristics depend only on the radial distance from the source. For the case of a moving monopole, the spectrum of the radiated field is determined by the Hankel-function. The spectrum contains energy mainly between the roots of the quadratic function k_{t}, where the argument of the Hankel function is real. Below and above the roots the amplitude decays exponentially. Most of the energy is concentrated around the two poles at $\omega_0 \frac{c^2 \pm cv}{c^2 - v^2}$. These are the dominant frequencies at the receiver position during the approaching and diverging of the moving source.

3.2 Sources moving at arbitrary direction

So far only sources, traveling parallel to the x-axis were considered. By utilizing the description for such sources we derived the formulation for an arbitrary directional source. Let's assume that the virtual source arrives at the x-axis at an angle of inclination φ.

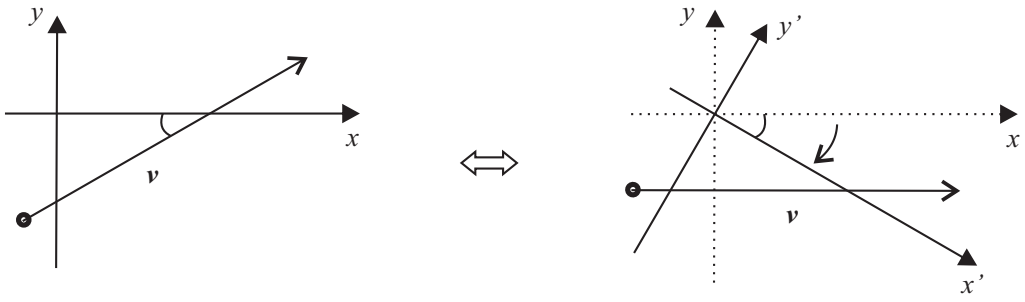

(a) (b)

Figure 3: The field of a source moving in arbitrary direction (a) can be derived from a source, moving parallel with x-axis in a rotated coordinate system (b)

By examining Fig. 3. we shall notice that the field, that the incident sound source generates on the x-axis, seen on figure part (a) is equal to the field of a source, moving parallel to the x-axis, taken on an axis, a rotated with an angle $-\varphi$, denoted by x'. This also holds for the y-axis. This means that the sound field of a source, with an arbitrary inclination angle can be derived from that of a parallel moving source with a simple coordinate rotation. The transformation matrix reads

$$\begin{bmatrix} x' \\ y' \end{bmatrix} = \begin{bmatrix} \cos\varphi & \sin\varphi \\ -\sin\varphi & \cos\varphi \end{bmatrix} \begin{bmatrix} x - x_{\mathrm{s}} \\ y - y_{\mathrm{s}} \end{bmatrix}$$

According to the aforementioned the spectrum of the field of a moving point source arriving at the x-axis with an angle of φ, located at $t = 0$ at $[x_{\mathrm{s}}\ y_{\mathrm{s}}\ 0]^{\mathrm{T}}$ is given by

$$P_{\mathrm{m}}(\mathbf{x},\omega) = -\frac{\mathrm{j}}{4v} H_0^{(2)}\left(-\mathrm{j}\hat{k}_t \sqrt{y'^2 + z^2}\right) \mathrm{e}^{-\mathrm{j}\hat{k}x'}, \tag{17}$$

where $\hat{k}_t = \sqrt{\hat{k}^2 - \left(\frac{\omega}{c}\right)^2}$, and x', y' is given by the matrix above.

Note that the same transform may be applied to the spatio-temporal description of a moving source, as given by [3] (5.60) in order to describe the field of a source, moving at arbitrary direction in the original coordinate system. This means that the pressure time history from a moving source moving with an inclination angle φ to the x-axis with an excitation time history $q(t)$ will read:

$$p(x, y, 0, t) = \frac{1}{4\pi} \frac{q(t-\tau)}{\Delta}, \tag{18}$$

with

$$\Delta = \sqrt{(x' - vt)^2 + y'^2(1 - M^2)} \tag{19}$$

and

$$\tau = \frac{M(x' - vt) + \Delta}{c(1 - M^2)}. \tag{20}$$

where $M = \frac{v}{c}$ denotes the Mach-number. This formulation will serve as a reference solution in the latter.

3.3 Moving sources in the wavenumber domain

In order to synthesize the ield of a moving source by SDM the spatial Fourier-transform of (17) is needed: $\tilde{P}(k_x, y, z, \omega) = \mathcal{F}\left(P_{\mathrm{m}}(\mathbf{x}, \omega)\right)$. The spectra are considered in the most relevant $z = 0$ plane only.

By using the modified Bessel representation of the moving source's spectrum the Fourier-transform to be evaluated is, by using the convolution theorem e.g [15]:

$$\frac{1}{2\pi v} \mathcal{F}_x \left(K_0(\hat{k_t}|y'|) \mathrm{e}^{-\mathrm{j}\hat{k}x'} \right) = \frac{1}{2\pi v} \mathcal{F}_x \left(K_0(\hat{k_t}|y'|) \right) * \mathcal{F}_x \left(\mathrm{e}^{-\mathrm{j}\hat{k}x'} \right). \tag{21}$$

The second term, by substituting the original coordinates and applying the Fourier-transform for an exponential:

$$\mathrm{e}^{-\mathrm{j}\hat{k}x'} = \delta(k_x - \cos\varphi\hat{k}) \mathrm{e}^{-\mathrm{j}\hat{k}(\sin\varphi(y - y_s) - \cos\varphi x_s)} \tag{22}$$

For the first term we use [8, (6.671,14)], exploiting that the function is even

$$\mathcal{F}_x \left(K_0(\hat{k_t}|x|) \right) = \frac{\pi}{\sqrt{k_x^2 + \hat{k}_t^2}}. \tag{23}$$

As $y' = -\sin\varphi x + (\sin\varphi x_s + \cos\varphi(y - y_s))$, we may use the similarity theorem and the shifting theorem ($\mathcal{F}(f(ax)) = \frac{F\left(\frac{k_x}{a}\right)}{|a|}$):

$$\mathcal{F}_x \left(K_0(\hat{k_t}|y'|) \right) = \frac{\pi}{\sin\varphi} \frac{\mathrm{e}^{\mathrm{j}\frac{k_x}{\sin\varphi}(\sin\varphi x_s + \cos\varphi(y - y_s))}}{\sqrt{(-\frac{k_x}{\sin\varphi})^2 + \hat{k_t}^2}}. \tag{24}$$

The convolution will sift out $k_x = k_x - \cos\varphi\hat{k}$. By substituting

$$\frac{1}{2v\sin\varphi} \frac{\mathrm{e}^{-\mathrm{j}\frac{\cos\varphi\hat{k} - k_x}{\sin\varphi}(\sin\varphi x_s + \cos\varphi(y - y_s))}}{\sqrt{\left(\frac{\cos\varphi\hat{k} - k_x}{\sin\varphi}\right)^2 + \hat{k_t}^2}} \mathrm{e}^{-\mathrm{j}\hat{k}(\sin\varphi(y - y_s) - x_s)}. \tag{25}$$

After rearranging the equation and using basic trigonometric identities the result for the description in the k_x domain is given

$$\tilde{P}_{\mathrm{m}}(k_x, y, 0, \omega) = \frac{1}{2v\sin\varphi} \frac{\mathrm{e}^{-\mathrm{j}\hat{k}\frac{y - y_s}{\sin\varphi}}}{\sqrt{\left(\frac{\cos\varphi\hat{k} - k_x}{\sin\varphi}\right)^2 + \hat{k_t}^2}} \mathrm{e}^{\mathrm{j}k_x \frac{\sin\varphi x_s + \cos\varphi(y - y_s)}{\sin\varphi}}. \tag{26}$$

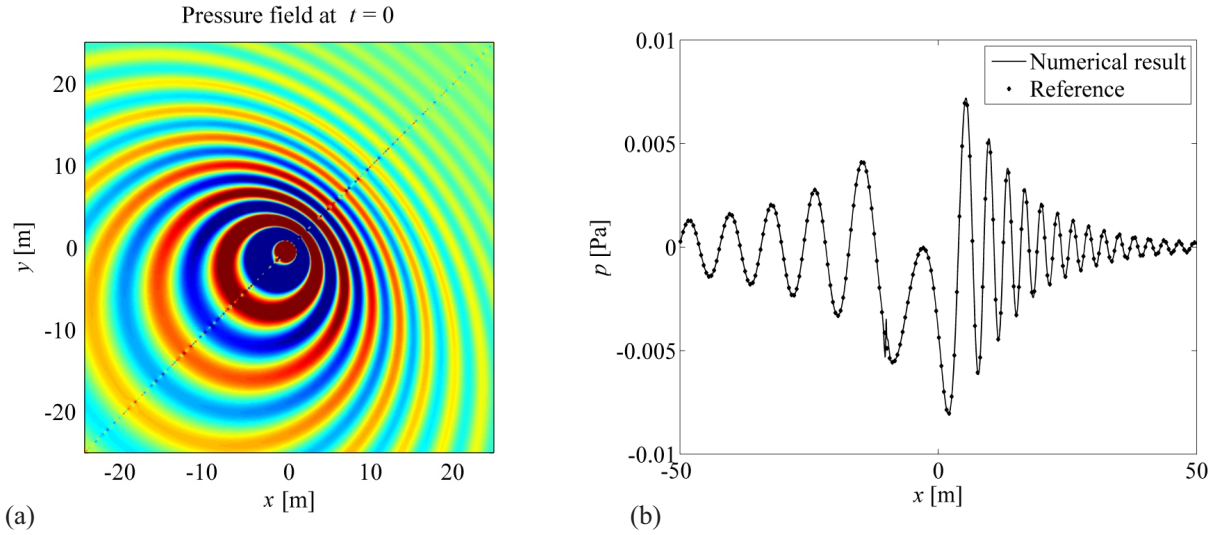

Figure 4: Snapshot of the real value of the sound field generated by a moving point source calculated in the wavenumber-frequency domain (a) and the field compared with the reference solution taken at $y = -10$ m (b).

Note, that this relation is not defined for $\varphi = 0$, thus for source moving parallel to the secondary source distribution. For these sources the spectrum is given by direct transform of equation (13), where only the exponential term is x-dependent

$$\tilde{P}_{\mathrm{par}}(k_x, y, 0, \omega) = -\frac{\mathrm{j}}{4v} H_0^{(2)}\left(-\mathrm{j}\hat{k}_t|y - y_s|\right) \mathrm{e}^{\mathrm{j}\hat{k}x_s}\delta(k_x - \hat{k}). \tag{27}$$

meaning that equation (26) converges to a Dirac-delta distribution.

In order to demonstrate the applicability of the theoretical results, the sound field of a moving source is presented in Fig. 4. The figure shows the result of direct numerical evaluation of equation (26) at the time origin. The point source travels with an angle of $45\,^\circ$, at a velocity of $200\ \mathrm{m/s}$, and radiates at 60 Hz. At the time origin the source is located at the spatial origin. The generated field examined at $y = -10$ m is compared with the spatio-temporal solution, as it was given by (18). The perfect matching with the reference solution indicates the validity of the results for both the temporal and the spatial Fourier-transform.

4 Synthesis of moving sources

4.1 Synthesis using wave field synthesis

In the previous section a general formulation for the sound field of a moving source was given both in spectral and wavenumber domain. In the followings the application of this description for sound field reproduction will be discussed.

As it was shown in section 2.1 for wave field synthesis in case of a planar secondary source distribution located at the $y = 0$ plane, the driving function equals to the y-directional derivative of the generated sound field at $y = 0$, given by equation (17), thus we need to evaluate expression

$$-\frac{\mathrm{j}}{4v}\frac{\partial}{\partial y}\left[H_0^{(2)}\left(-\mathrm{j}\hat{k}_t\sqrt{((y-y_s)\cos\varphi - (x-x_s)\sin\varphi)^2 + z^2}\right)\mathrm{e}^{-\mathrm{j}\hat{k}((x-x_s)\cos\varphi + (y-y_s)\sin\varphi)}\right]_{y=0}. \tag{28}$$

.

The derivation can be carried out analytically, using the chain rule, and that $\frac{\partial}{\partial z}H_0^{(2)}(z) = -H_1^{(1)}(z)$ according to [6] p.605, (11.93) and [2] p.358, (9.1.6). The driving function using the derivative at $y = 0$ then reads:

$$D(x,0,z,\omega)_{\text{planar}} = \frac{\mathrm{e}^{-\mathrm{j}\hat{k}x'}}{2v}(\hat{k}\sin\varphi H_0^{(2)}(-\mathrm{j}\hat{k}_t r_t') - \frac{\hat{k}_t\cos\varphi y'}{r_t'}H_1^{(2)}(-\mathrm{j}\hat{k}_t r_t')) \tag{29}$$

where $x' = \cos\varphi(x - x_s) - \sin\varphi y_s$, $y' = -\sin\varphi(x - x_s) - \cos\varphi y_s$ and $r_t' = \sqrt{y_s'^2 + z^2}$. The reproduced field then will read in a fixed observer position

$$P(x,y,z,\omega) = \iint_{-\infty}^{\infty} D(x_0,0,z_0,\omega)_{\text{planar}} G(x - x_0, y, z - z_0, \omega)\mathrm{d}x_0\mathrm{d}z_0 \tag{30}$$

The driving functions would ensure perfect reconstruction in the $y > 0$ half-space by applying an ideal continuous, infinite plane as a secondary source distribution.

In order to obtain the WFS driving functions for linear secondary source distribution the integration along z-direction in integral (30) is carried out. This can be done by first applying large-argument exponential approximation for the Hankel-functions as given by [2] p.364, (9.2.4):

$$H_1^{(2)}(z) \approx -\sqrt{\frac{2}{\mathrm{j}\pi}}\frac{\mathrm{e}^{-\mathrm{j}z}}{\sqrt{z}}, \qquad H_0^{(2)}(z) \approx \sqrt{\frac{2\mathrm{j}}{\pi}}\frac{\mathrm{e}^{-\mathrm{j}z}}{\sqrt{z}}, \tag{31}$$

Thereafter the integrate of the oscillatory function is obtained by applying the method of stationary phase, suggesting that the point source at the stationary point and its immediate surroundings give the major contribution to the integral [5]. As for the case of a stationary virtual source the stationary phase point is found at $z = 0$. The obtained $2\,\frac{1}{2}$-dimensional driving function reads:

$$D(x,\omega)_{\text{WFS}} = \frac{1}{v}\sqrt{\frac{r}{k|y'| - \mathrm{j}\hat{k}_t r}}\left(\sqrt{\frac{\hat{k}_t}{\mathrm{j}}}\cos\varphi + \sqrt{\frac{\mathrm{j}}{\hat{k}_t}}\hat{k}\sin\varphi\right)\mathrm{e}^{-\hat{k}_t|y'| - \mathrm{j}\hat{k}x'}, \tag{32}$$

and the synthesized field reads in the plane of synthesis

$$P(x,y,0,\omega) = \int_{-\infty}^{\infty} D(x_0,\omega)_{\text{WFS}} G(x - x_0, y, 0, \omega)\mathrm{d}x_0. \tag{33}$$

This driving function is still dependent on $r = \sqrt{(x - x_0)^2 + y^2}$, which is the distance between the observer position and the actual secondary source position. In order to achieve perfect synthesis along a reference line instead of a reference point the same procedure is carried out as it is given in [13] for stationary virtual sources. A further stationary point has to be found, where the exponential in integral (33) is stationary, thus its derivative is zero. This stationary point reads

$$r_0 = |y_{\text{ref}}|\sqrt{\frac{k^2}{k^2 - (\hat{k}\cos\varphi - \mathrm{j}\hat{k}_t\sin\varphi)^2}}. \tag{34}$$

This wavenumber-dependent distance, substituted in place of r is now independent from x, therefore ensures an approximately perfect synthesis on a fixed $y = y_{\text{ref}}$ line. All three approximations are valid in the far-field, meaning that synthesis will be correct only relatively far from the secondary source distribution.

Note, that for sources, moving parallel to the secondary sources ($\varphi = 0$) $r_0 = -\mathrm{j}|y_{\text{ref}}|\frac{k}{\hat{k}_t}$ and the driving function simplifies to

$$D(x,\omega)_{\text{WFS,par}} = \frac{1}{v}\sqrt{\frac{|y_{\text{ref}}|}{|y_s| + |y_{\text{ref}}|}}\mathrm{e}^{-\hat{k}_t|y_s| - \mathrm{j}\hat{k}(x - x_s)}. \tag{35}$$

4.2 Synthesis using spectral division method

The spectral-wavenumber description of the sound field of a moving sound source the application for sound field synthesis is very straightforward. As it was given by (7) the spectrum of driving function is the ratio of the spectrum of generated field, given by (26) and (27) and the spectrum of a stationary monopole at the origin, described by equation (8), both written on the reference line y_{ref}. Based on the foregoing the spectrum of the driving function for a source, moving at direction φ will read:

$$\tilde{D}(k_x,\omega)_{\mathrm{SDM}} = \frac{\tilde{P}_{\mathrm{m}}(k_x, y_{\mathrm{ref}}, 0, \omega)}{\tilde{G}(k_x, y_{\mathrm{ref}}, 0, \omega)} \tag{36}$$

where the spectra are given by equation (26) and (8).

For a source, moving parallel to the secondary source distribution the driving function reads

$$\tilde{D}(k_x,\omega)_{\mathrm{SDM,par}} = \frac{1}{v}\frac{H_0^{(2)}\left(-\mathrm{j}\sqrt{\hat{k}^2-k^2}|y_{\mathrm{ref}}-y_s|\right)}{H_0^{(2)}\left(-\mathrm{j}\sqrt{k_x^2-k^2}|y_{\mathrm{ref}}|\right)}\mathrm{e}^{-\mathrm{j}\hat{k}x_s}\delta(k_x-\hat{k}). \tag{37}$$

To obtain the driving function in the spatial-spectral domain spatial inverse Fourier-transformation of the spectra is needed. For sources with arbitrary direction no analytical inverse-transform were found. For a parallel moving source the transform reads:

$$D(x,\omega)_{\mathrm{SDM,par}} = \frac{1}{v}H_0^{(2)}\left(-\mathrm{j}\sqrt{\hat{k}^2-k^2}|y_{\mathrm{ref}}-y_s|\right)\mathrm{e}^{-\mathrm{j}\hat{k}x_s}\int_{-\infty}^{\infty}\frac{\mathrm{e}^{-\mathrm{j}k_x x}}{H_0^{(2)}\left(-\mathrm{j}\sqrt{k_x^2-k^2}|y_{\mathrm{ref}}|\right)}\delta(k_x-\hat{k})\mathrm{d}k_x. \tag{38}$$

We can exploit the sifting property of the Dirac-delta function, which will sift out $k_x = \hat{k}$ as the result of integration. As $k_t|_{k_x=\hat{k}} = \hat{k}_t$ the resulting driving function is given by

$$D(x,\omega)_{\mathrm{SDM,par}} = \frac{1}{v}\frac{H_0^{(2)}\left(-\mathrm{j}\hat{k}_t|y_{\mathrm{ref}}-y_s|\right)}{H_0^{(2)}\left(-\mathrm{j}\hat{k}_t|y_{\mathrm{ref}}|\right)}\mathrm{e}^{-\mathrm{j}\hat{k}(x-x_s)}. \tag{39}$$

It can be easily proven, that by applying the large argument approximation for the Hankel function in equation (39) the driving function takes the same form as it was obtained by WFS, given by equation (35), meaning that in the far-field the two techniques lead to exactly the same result.

5 Numerical examples and comparison

In this chapter several examples given for the application of the presented sound field reproduction techniques. All the simulation results were carried out in the time domain, by using the numerical inverse Fourier transform of the driving functions' spectra, obtained by the presented methods. By using the spatio-temporal driving functions $d(x,t) = \mathcal{F}^{-1}\left(D(x,\omega)\right)$ the reproduced sound field were calculated as

$$p(x,y,0,t) = \sum_{x_0}\frac{d(x_0, t-\frac{r}{c})}{r}, \tag{40}$$

where $r = \sqrt{(x-x_0)^2+y^2}$. For all the presented comparison the reference was the spatio-temporal description of the sound field of a moving source, obtained by the direct evaluation of equation (18).

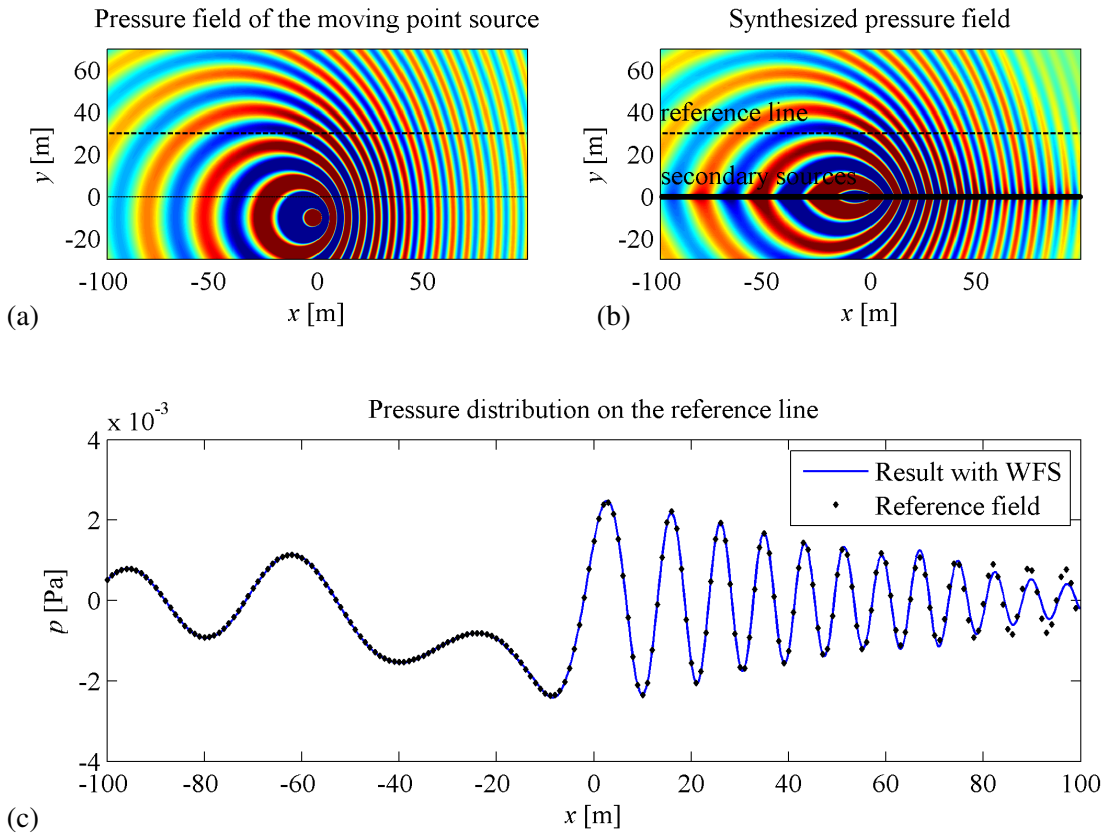

Figure 5: Snapshot of pressure field of the original moving source (a), snapshot of the synthesized sound field by SDM (b) and the comparison of result of WFS and the reference solution taken at the reference line (c).

5.1 Sources moving parallel to the secondary sources

Figure 5 shows the synthesis of a sound source, moving parallel to the secondary source distribution. In this case both the WFS and SDM gives an analytical solution in the spatial-frequency domain, thus only temporal numerical inverse-transform is needed. In the current simulation the sound field, generated by a point source, moving with a velocity $200\ \mathrm{m/s}$, oscillating at $20\ \mathrm{Hz}$ is investigated. The snapshots are taken at the time origin, when the source is located at $[0, -5, 0]^{\mathrm{T}}\ \mathrm{m}$. The reference line is set to $30\ \mathrm{m}$. Simulations are carried out by evaluating (40), where $d(x,t)$ are the numerical inverse transform of equations (35) and (39). It can be seen, that not only the SDM, which serves as a reference solution by definition, but also the WFS, which employs far-field approximations gives a perfect synthesis on the reference line. Minor amplitude errors may be observed on the figure for great x values. This is partly due to the diffraction, caused by the secondary source truncation and also due to the fact that in this part of the sound field the truncated secondary source elements would have a great contribution.

In the aspect of virtual reality applications not only the spatial distribution, but also the time history of the generated sound field is of great importance. Figure 6 shows the time history of the reproduced sound field, measured at $[0, y_{\mathrm{ref}}, 0]$. Here the virtual source moves again at the velocity $200\ \mathrm{m/s}$, oscillating at $50\ \mathrm{Hz}$, $\mathbf{x}_s = [0, -1, 0]^{\mathrm{T}}$ and $y_{\mathrm{ref}} = 3$. Figure 6 (a) shows, that SDM also provides a perfect reconstruction of the original source's time history in front of the secondary source array. This is also confirmed by 6 (b), which spectogram-like diagram shows the instantaneous frequency of the measured signal as the function of time. The results were obtained by assuming a complex linear dependency between the neighbouring samples

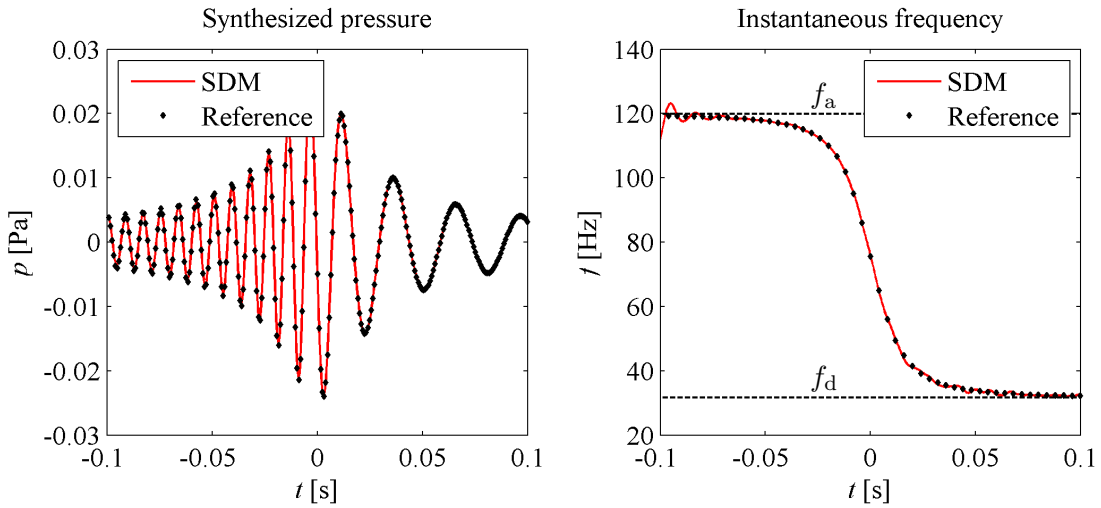

Figure 6: Time history (a) and instantaneous frequency history (b) of the reference, and the synthesized sound field

in the measured time history. From this, the instantaneous phase change, and thus the frequency can be calculated. Besides several numerical errors the figure indicates the perfect reconstruction of the perceived Doppler-effect. In the figure also the theoretical dominant frequencies are indicated with dashed black lines for approaching and diverging. These are calculated as $f_{\mathrm{a,d}} = f_0 \frac{c^2 \pm cv}{c^2 - v^2}$, which are in this case 31.6 Hz and 119.88 Hz.

5.2 Sources moving in arbitrary direction

In case for a point source, moving in arbitrary $\varphi \neq 0$ direction WFS still gives a result in the spatial-frequency domain, but due to its complexity the driving function for SDM can be calculated only numerically. Numerical calculation of the spatial Fourier transform may lead to several undesired artifacts.

The first problem is caused by aliasing which is caused by the discretization of the driving function spectrum, which belongs to the sound field, generated by periodically repeating sources, moving in the same direction. The distance between these sources is defined by $\mathrm{d}k_x = L$, the prescribed wave-number resolution, L is the spatial length, where the driving function is to be calculated. If the resolution is not fine enough, the overlapping of the field of these sources may have a significant effect, occuring as spatial aliasing. To avoid this, in the present example the spectrum of the driving function is calculated oversampled and the final resolution is achieved by low-pass filtering and decimating.

The second problem is that the reciprocal of the spectrum of the stationary monopole grows exponentially with k_x, which can cause a blow up at the evanescent region due to numerical errors. This is a well-known artifact in the field of Near Field Acoustic Holography . To avoid this numerical regularization is needed. In the present example a low-pass filter is applied with a smoothed transition at $k_x = \frac{\omega}{c}$.

The efficiency of the derived driving functions are presented here through the example for a point source, moving uniformly with velocity 200 $\mathrm{m/s}$, oscillating at 20 Hz, arriving to the x-axis with an angle of inclination 30°. The source is located in the time origin at $\mathbf{x}_s = [0, -5, 0]^{\mathrm{T}}$, and the refrence line is set to $y_{\mathrm{ref}} = 10$ m. Figure 7 (a) shows the targeted sound field by evaluating equation (18). In part (b) of figure 7 a snapshot, taken at $t = 0$ of the generated sound field by using linear WFS can be seen. The visible difference between the amplitude distributions predictes that the directivity of the finite secondary source array also has an effect on the radiated sound field, however thes artifacts have not been investigated yet in details.

Figure 7 (c) shows the result of synthesis, using WFS with a planar secondary source distribution by implementing equation (29), while in figures 7 (d) and (e) the result of synthesis with linear secondary source

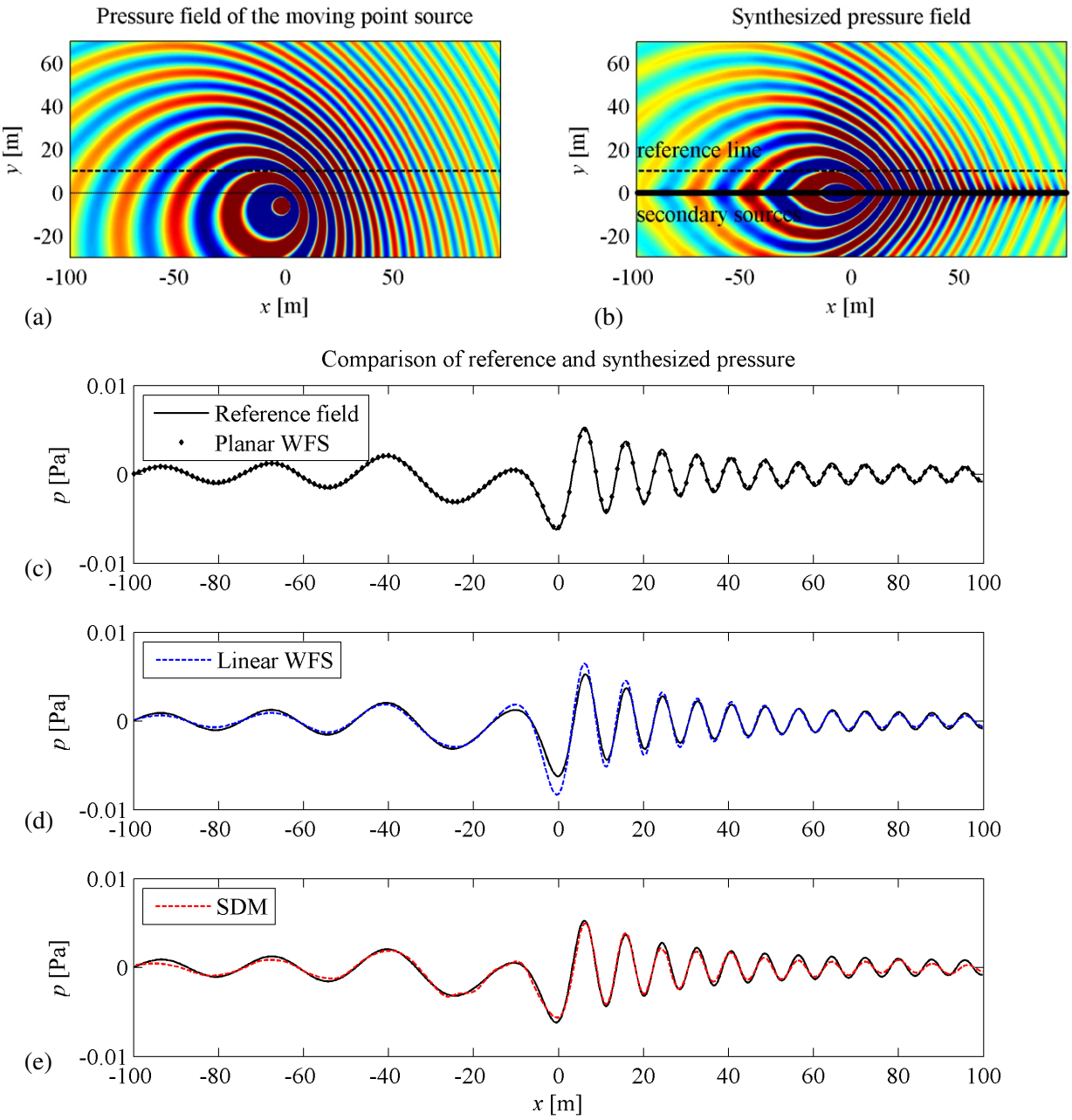

Figure 7: The reproduction of a sound source, movint at $\varphi = 30°$ to the x-axis at $t = 0$: The target sound field (a), snapshot of synthesized sound field using WFS (b), cross-section of the synthesized sound field along the reference line using WFS with planar secondary source distribution (c), linear secondary source distribution (d) and SDM (e)

using WFS and SDM can be seen by apply driving functions (32) and (36).

As expected, the result of synthesis using a planar secondary source distribution perfectly match the reference sound field not only on the reference line, but at any point of the synthesis plane. For case of WFS and SDM slight amplitude errors occur in both cases. For WFS the dreatest differences may be observed around $x = 0$. These errors may occur due to the approximations, applied in the derivation for the driving functions. As SDM should ensure a perfect synthesis on $y = y_{\text{ref}}$ the observed errors originate from the numerical spatial and temporal Fourier-transforms. Besides these amplitude errors both techniques, applying linear secondary array result in a phase-correct synthesis on the reference line, which fact confirmes the validity of

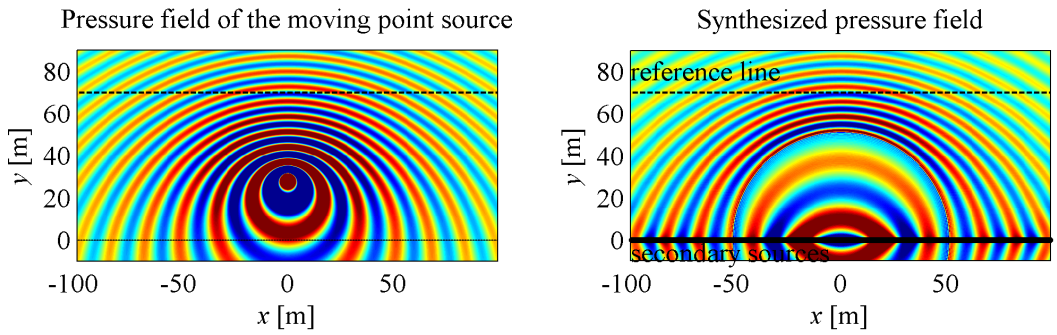

Figure 8: Synthesis of a point source, moving perpendicular to the secondary source distribution after crossing the secondary sources

the theoretical results, given in the previous chapters.

For sources, moving at arbitrary direction the time history of the synthesized field were not investigated, because in this case at a given time instant the virtual source will cross the secondary source distribution. The driving functions presented here are not capable yet to handle this situation, as after the crossing of the virtual source acoustical focusing would be needed. As a result for a given time instant only those part of the sound field will be synthesized correctly, where the scalar product of the normal vector a the point of the wave front to be synthesized and the secondary source distribution is positive. The synthesized sound field of a point source moving perpendicular to the secondary source distribution can be seen in figure 8 after the virtual source has crossed the secondary source line.

6 Conclusion

In the present contribution a thorough treatise on the description and synthesis of moving sound sources was given. The research was motivated by the fact, that so far only mathematically incorrect solutions have been given in the related literature.

First, based on the spectral description of a sound source, moving parallel to the x-axis we gave a spectral description for a source moving at arbitrary direction. By finding an analytical expression for the spatial Fourier-transform we extended this description to the spectral-wavenumber domain. By utilizing the spectral description a compact analytical formula was found for the synthesis of moving sources using traditional wave field synthesis applying both planar and linear secondary source distribution. Based on the presented wavenumber representation of the targeted sound field an explicit driving function was given to utilize the spectral division method. In case of a sound source, moving parallel to the secondary source distribution the spatial driving function for the spectral division method was given, by analytically inverse-transforming the driving functions in the wavenumber domain.

Numerical simulation results confirmed that the given driving functions for both techniques are correct. There are however still several possibilities for further development. First, as it could be seen the obtained driving functions result in correct synthesized sound field only in case of non-focusing synthesis. In order to handle sources, crossing the secondary source distribution acoustical focusing should be involved. Secondly, in the current study only sources, oscillating at a single frequency were presented. Synthesis of sources with arbitrary excitation signal is possible with the WFS and SDM driving functions shown here, however it is yet computationally expensive. The efficient implementation of driving functions for virtual sources with arbitrary time excitation history is also an opened question.

References

[1] Gerzon Michael A., *Periphony: With-height sound reproduction*, Journal of the Audio Engineering Society **21** (1973), 2–10.

[2] Milton Abramowitz and Irene A. Stegun, *Handbook of mathematical functions with formulas, graphs and mathematical tables*, United States Department of Commerce, 1972.

[3] Jehns Ahrens, *Analytic methods of sound field synthesis*, Springer, 2012.

[4] Jens Ahrens and Sacha Spors, *An analytical approach to sound field reproduction using circular and spherical loudspeaker distributions*, Acta Acustica united with Acustica **94** (2008), 988–999.

[5] Berkhout A.J., de Vries D., and Vogel P., *Acoustic control by wave field synthesis*, Journal of the Acoustical Society of America **93** (1993), no. 5, 2764–2778.

[6] George Arfken, *Mathematical methods for physicists*, third ed., Academic Press, 1985.

[7] Andreas Franck, Andreas Graefe, Thomas Korn, and Michael Strauss, *Reproduction of moving sound sources by wave field synthesis: An analysis of artifacts*, 32nd International Conference of the AES: DSP For Loudspeakers, 2007.

[8] I.S. Gradshteyn and I.M. Ryzhik, *Table of integrals, series, and products*, Elsevier, 2007.

[9] Sacha Spors Jens Ahrens, *Reproduction of moving virtual sound sources with special attention to the doppler effect*, Audio Engineering Society Convention 124 (Amsterdam, The Netherlands), 2008.

[10] ———, *Sound field reproduction using planar and linear arrays of loudspeakers*, IEEE Transactions on Audio, Speech and Language Processing **18** (2010), no. 8, 2038–2050.

[11] Richard A. Handelsman Norman Bleinstein, *Asymptotic expansions of integrals*, Holt, Rinehart and Winston, 1975.

[12] Jens Ahrens Sacha Spors, Rudolf Rabenstein, *The theory of wave field synthesis revisited*, Audio Engineering Society Convention Paper, May 2008, AES 124th Convention, Amsterdam, The Netherlands.

[13] Evert Walter Start, *Direct sound enhancement by wave field synthesis*, Ph.D. thesis, Delft University of Technology, 1997.

[14] Edwin Verheijen, *Sound reproduction by wave field synthesis*, Ph.D. thesis, Delft University of Technology, 1997.

[15] Earl G. Williams, *Fourier acoustics: Sound radiation and nearfield acoustical holography*, Academic Press, 1999.